ISSN 0208-7774 TRIBOLOGIA 1/2023 p. 65–75
DOI: 10.5604/01.3001.0016.2934

Marek SZEWCZYK[*], Krzysztof SZWAJKA[**]

ANALYSIS OF FRICTION FORCES IN THE PROCESS OF FORMING MOULDING MASS

ANALIZA TARCIA ZEWNĘTRZNEGO W PROCESIE FORMOWANIA MAS FORMIERSKICH

Key words: coefficient of friction, stresses, strain gauges, forming.

Abstract: Accelerated wear of the moulds' inner surface used in forming loose masses contributes to its frequent replacement or regeneration. This wear is indirectly influenced by the high pressure accompanying the compaction process, but the main cause of accelerated wear is the friction that occurs between the die and the compacted medium. Knowing that the value of the internal pressure in the moulded medium changes with the change of the distance from the punch, in order to properly understand the phenomena accompanying the friction that occurs in the mould during the pressing process, its characteristics must be determined. The paper analyses the distribution of forming pressure inside the mould during the compaction of high-silica sand. The deformation on the die surface was measured using strain gauges, and x-ray tomography was used to visualise the compaction of high-silica sand during the compaction process. The usefulness of an indirect method for measuring the friction coefficient based on the analysis of die deformation has been demonstrated.

Słowa kluczowe: współczynnik tarcia, naprężenia, tensometry, formowanie.

Streszczenie: Przyśpieszone zużycie powierzchni wewnętrznej form, stosowanych w procesach formowania mas sypkich, przyczynia się do częstej jej wymiany lub regeneracji. Na zużycie to pośrednio wpływa wysokie ciśnienie towarzyszące procesowi zagęszczania, ale główną przyczyną mającą wpływ na przyspieszone zużycie jest tarcie, które występuje pomiędzy matrycą a medium zagęszczanym. Wiedząc, że wartość ciśnienia wewnętrznego w medium formowanym zmienia się wraz ze zmianą odległości od stempla, dla prawidłowego zrozumienia zjawisk towarzyszących tarciu, które zachodzi w formie podczas procesu prasowania, należy więc określić jego charakterystykę. W pracy przeanalizowano rozkład ciśnienia formującego wewnątrz formy podczas zagęszczania piasku wysokokrzemionkowego. Odkształcenie na powierzchni matrycy mierzono za pomocą tensometrów. W celu zobrazowania zagęszczania piasku wysokokrzemionkowego podczas procesu zagęszczania zastosowano tomografię rentgenowską. Wykazano przydatność zastosowania pośredniej metody do pomiaru współczynnika tarcia opartej na analizie odkształceń matrycy.

INTRODUCTION

Currently, bulk medium compaction processes are used in many industries, an example of which is the foundry industry, in which sand moulds are used. Another example is powder metallurgy **[L. 1, 2]**, with the help of which it is possible to produce construction materials, make elements of machine parts, or produce cutting tool blades. Manufacturers using this production method face a number of problems related to obtaining a finished product that would be characterised by adequate strength while maintaining minimal wear of the mould surface due to friction and high pressures. Granular materials include granular soils, filling materials in earth-rock structures **[L. 3]** and wood

[*] ORCID**:** 0000-0002-3622-6613. Rzeszow University of Technology, The Faculty of Mechanics and Technology, Kwiatkowskiego Street 4, 37-450 Stalowa Wola, Poland.
[**] ORCID: 0000-0002-1038-1148. Rzeszow University of Technology, The Faculty of Mechanics and Technology, Kwiatkowskiego Street 4, 37-450 Stalowa Wola, Poland.

materials for producing pellets **[L. 4]**. The physical properties of bulk materials affect the correlation between grain size distribution and compacted products' physical and mechanical properties.

As mentioned earlier, the most important problem resulting from the compaction of the loose medium is the non-uniformity of the compaction of the final product material. This involves movement between the compacted material particles and the matrix surface. As a result, apart from the obvious interaction forces between the particles, the compaction process is accompanied by friction forces between the particles, the bottom of the punch and the walls of the die **[L. 5, 6]**. Since the distribution of these forces is uneven over the entire surface of the die, the value of the forming pressure also changes in the entire volume of the material.

Indirect measurement methods can be used to determine the value of the moulding pressure distribution inside the mould by measuring the deformations on the outer surface of the mould. The most common method of measuring deformations is the method based on resistance strain gauges **[L. 7]**. This method is often used due to its high accuracy and low cost. The advantage of this method is the possibility of measuring the strain with more than one strain gauge. Another quite often used method of measuring deformations is the method using piezoelectric sensors **[L. 8]**. This method, similar to measurement using the strain gauge method, requires direct contact with the sensor with the surface of the tested object. The advantage of this method is that the piezoelectric sensor, unlike strain gauges, is reusable. Another method used to measure deformation is a non-contact system for 3D deformation analysis and Digital Image Correlation (DIC), which consists of superimposing photos taken at different angles using a set of cameras, resulting in a graphic map of deformation **[L. 9, 10]**. This method allows us to determine the deformation distribution on the tested element's entire surface.

The compressibility of bulk materials, particularly sands, is favoured by higher initial porosity, increasing grain angularity, and decreasing internal grain strength **[L. 11, 12]**. Large grain size and high initial porosity result in increased stress concentration in contact between adjacent particles **[L. 11, 13]**. The initial grain size also determines the value of contact stresses. The grain fraction's reduced size range due to the coordination number's low value leads to an increase in contact stresses **[L. 13]**. High-stress values exceed the critical stresses in the particles of the pressed material, leading to their cracking, which increases further densification as a result of grain rearrangement **[L. 11, 12]**. This phenomenon is particularly noticeable when compacting particles from brittle materials, for example, sand. Sands deformed under high-pressure conditions show trans-crystalline cracks spreading from the grain contact points **[L. 11, 14]**.

MATERIAL AND METHODOLOGY OF RESEARCH

The loose material used for the tests was quartz sand used to produce castings. Quartz sand consists mainly of quartz arenite, which is

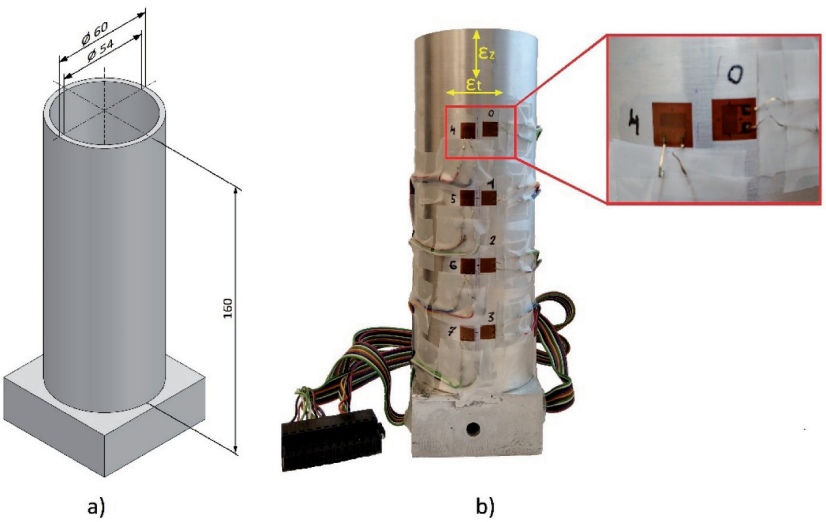

Fig. 1. a) the form used in the tests, b) the method of sticking strain gauges on the surface of the form
Rys. 1. a) forma zastosowana w badaniach, b) sposób naklejenia tensometrów na powierzchni formy

a clastic sedimentary rock with a grain size of 0.0625 mm to 2 mm. High-silica sand contains a high proportion of silica (over 95%). The sand used in the tests was subjected to a sieve analysis, thanks to which fractions of similar size of individual sand grains were obtained, ranging from about 0.4 to 0.315 mm.

During the sand-pressing process, a pipe-shaped mould was used to analyse the distribution of the external friction force inside the mould. The geometric dimensions of the mould prepared for testing are shown in **Figure 1**. The pipe and the base were made of aluminium alloy EN AW-2017(A) with good tensile and fatigue properties, and both of these elements were joined together by TIG welding. Selected physical and mechanical properties of the EN AW-2017(A) alloy are presented in **Table 1**.

Table 1. Selected physical and mechanical properties of EN AW-2017(A) aluminium alloy [L. 15]
Tabela 1. Wybrane właściwości fizyko-mechaniczne stopu aluminium EN AW-2017(A) **[L. 15]**

Properties	Unit	Value
HB hardness	–	110
Density	g/cm	2.79
Poisson's ratio	–	0.33
Thermal expansion coefficient	°C	22.9 × 10
Resistance	nΩm	51
Young's modulus	MPa	72500

The research was conducted in two stages. As part of the first stage of the research, deformations (ε) formed on the external surface of the mould during the pressing process were measured and recorded. In the second stage of the research, the distribution of pressure inside the mould (p(z) as a function of mould height (z)) depending on the distance from the punch was determined. A method based on resistance strain gauges was used in the tests related to the measurement of stress distribution during the pressing process. The choice of this measurement method was dictated by the fact that it belongs to the accurate and cheap methods of determining stresses based on strains. The arrangement of strain gauges on the surface of the mould was selected in such a way as to record the change in the deformation value over the entire height of the mould. Due to the fact that strain gauges capable of measuring the strain distribution in one direction were used in the tests, two strain gauges were used, glued next to each other and rotated by 90 degrees to each other. This made it possible to measure the strain distribution in both the axial (εz) and tangential (εt) directions on the outer surface of the mould, as shown in **Figure 1**.

Measurements of deformations occurring on the outer surface of the mould during the bulk medium compaction process were carried out on a stand consisting of the NI cDAQ-9132 controller and the NI 9236 strain measurement module. Strain gauges glued to the mould surface were connected to this module (**Fig. 1**). TF-5/350 film extensometers were used, the parameters of which are presented in **Table 2**. Quasi-static compaction (pressing) of the loose medium was carried out on a Zwick/Roell Z100 testing machine (**Fig. 2**). A mould was mounted in the lower holder of the testing machine, while a punch was mounted in the upper one. During the experiment, the force and displacement of the punch were recorded with a frequency of 50 Hz. The punch speed was 10 mm/min. The mould punch was loaded so as to obtain a sand pressure of 15 MPa.

Table 2. Parameters of the TF-5/350 strain gauge
Tabela. 2. Parametry tensometru TF-5/350

Parameter	Unit	Value
Resistance	Ω	350 ±0.2%
Width	mm	5.0
Length	mm	8.5
Thickness	μm	60
Maximum amperage	mA	50
Operating temperature range	°C	−40 – 200
Fatigue strength	–	n > 107 for ε = 0.1%
Maximum deformation	%	ok. 4
Deformation sensitivity coefficient k	–	2.1 – 2.2
k-factor tolerance, %	%	0.5

The visualisation of changes in sand compaction was carried out using an X-ray tomograph, which allowed the observation of the behaviour of the loose medium inside the mould based on the displacements of reference points, which were rows of lead balls with a diameter of 4 mm, as shown in **Figure 3** (section A-A). The distance between the beads layers was about 15 mm.

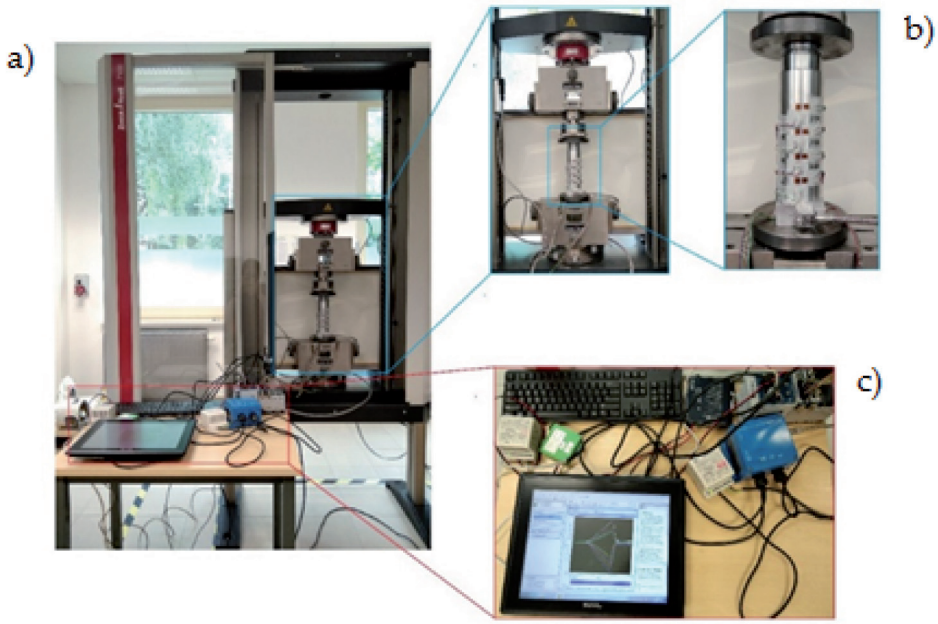

Fig. 2. Stand for measuring deformations: a) a mould mounted on a testing machine, b) a view of the mould in the process of sand pressing, c) measuring equipment

Rys. 2. Stanowisko do pomiaru odkształceń: a) forma zamontowana na maszynie wytrzymałościowej, b) widok formy w procesie prasowania piasku, c) aparatura pomiarowa

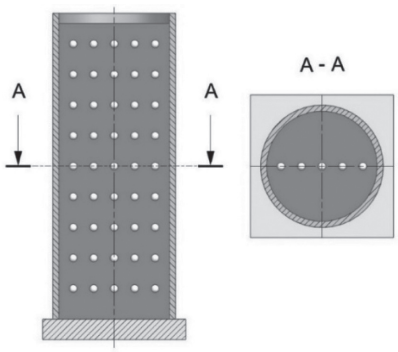

Fig. 3. Diagram of the arrangement of the balls in the die

Rys. 3. Schemat rozmieszczenia kulek w matrycy

The mould shown in **Figure 3** was X-rayed and photographed using a General Electric phoenix v|tome|xm X-ray tomograph. In order to correctly estimate the compaction inside the mould as a result of sand pressing, it was necessary to know the displacement values of individual layers of balls. Therefore, the X-ray process was carried out twice, i.e., before and immediately after the compaction process. The X-ray stand used for the tests is shown in **Figure 4**.

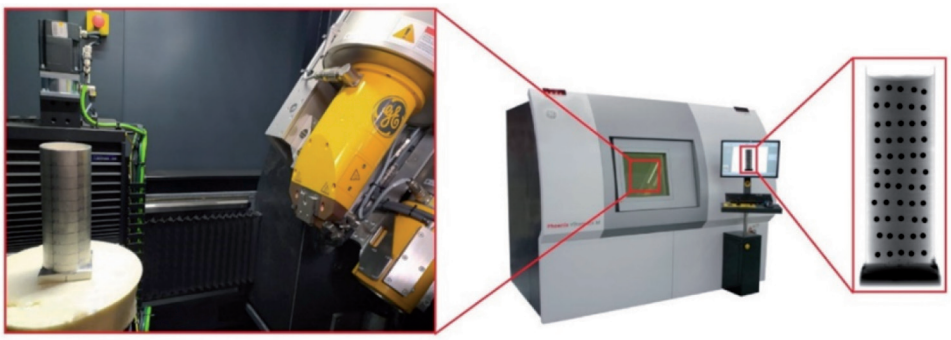

Fig. 4. X-ray test stand: a) placing the mould on the rotary table of the X-ray tomograph, b) X-ray tomograph phoenix v|tome|x m by General Electric, c) X-ray image of the mould

Rys. 4. Stanowisko do badań rentgenowskich: a) ustawienie formy na obrotowym stole tomografu rentgenowskiego, b) tomograf rentgenowski phoenix v|tome|x m firmy General Electric, c) zdjęcie rentgenowskie formy

DISCUSSION

The recorded values of die surface deformations during the pressing of quartz sand are shown in **Fig. 5**. The largest tangential deformations (εt) were recorded near the punch surface (no. 0). Then, the values of tangential deformations of the die walls decreased exponentially with the distance from the punch surface. A different situation occurred in the case of axial strains (ε_z). The highest value of axial deformation was reached in the place farthest from the punch (no. 7). This is understandable because the external friction forces are "added up" as you move away from the punch. As in the case of the values of tangential deformations of the die walls, the changes in the values were exponential

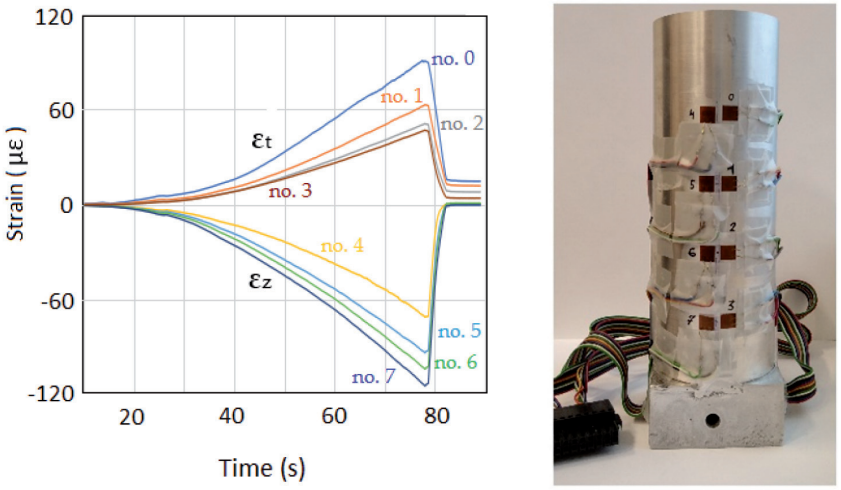

Fig. 5. Strain distribution along the height of the die during the compaction of the high-silica sand
Rys. 5. Rozkład odkształceń na wysokości matrycy podczas zagęszczania piasku kwarcowego na kierunku osiowym (ε_z) oraz na kierunku stycznym (ε_t)

Figure 6 shows the displacement of the lead balls during quartz sand compression. During these studies, as well as the analysis of the literature, it was found that the value of the pressure inside the mould changes as a function of the change in the distance from the punch. This hypothesis was confirmed by the results of the research carried out, in which changes in the density of the bulk medium during the pressing process were analysed.

Figure 6 shows images illustrating the balls' positions before the pressing process (a) and after the pressing process (b). They are superimposed on each other. The recorded changes in the position of the balls prove a different nature of powder compaction at the height of the matrix. A diagram quantifying the displacement of the balls after the pressing process is shown in **Figure 7**. Both the value of the displacement (xi) and the height of the mould (hi) are expressed in millimetres.

The dependence of the changing value of the displacement of the balls, depending on the distance from the punch surface, can be described using an exponential function. The largest displacement of the balls was observed closest to

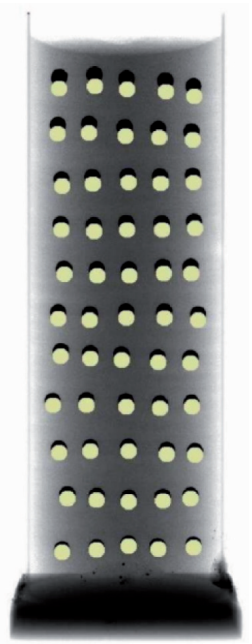

Fig. 6. Computed tomography scan of the position of the balls before the (black outline) and after the (yellow outline) compaction process
Rys. 6. Zdjęcie wykonane tomografem komputerowym ilustrujące położenie kulek przed (czarny kolor) i po (żółty kolor) procesie zagęszczenia

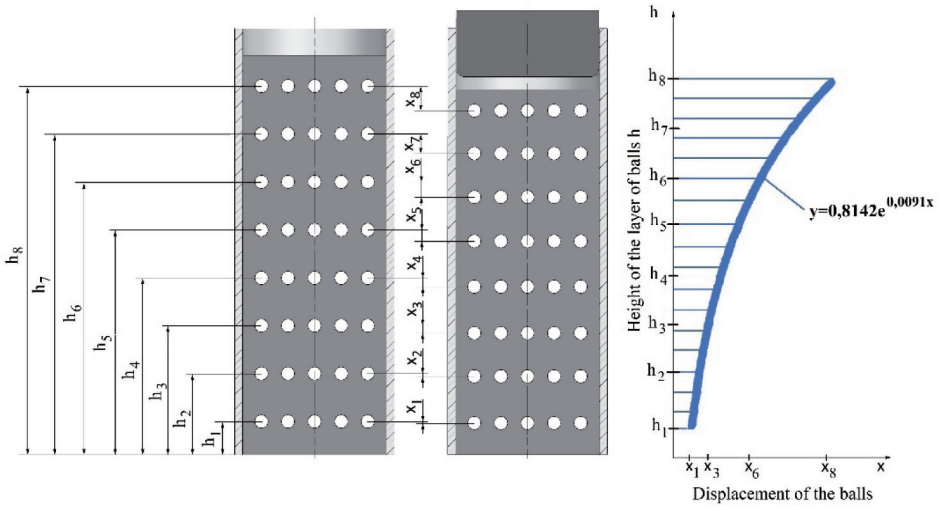

Fig. 7. Distribution of lead balls (a) before and (b) after the pressing process, and (c) function of the displacement of the ball through the die height

Rys. 7. Rozkład kulek ołowianych (a) przed i (b) po procesie prasowania oraz (c) funkcja opisująca przemieszczenie kulek w funkcji wysokość formy – p(z)

the surface of the punch, and with the distance from this surface, the displacement distance decreased. This unambiguously determines the variable nature of the compaction of the loose material inside the mould and thus confirms the variable nature of the pressure distribution inside the mould during the pressing process.

The force exerted by two bodies in contact that opposes their relative motion is called the force of friction T. The force of friction is tangential to the surface of contact, acts on each body and is in the opposite direction to its velocity relative to the other body (**Fig. 8**). The source of the friction force is the interaction between the particles of the bodies in contact. If the bodies do not move relative to each other, the force of friction is called static friction. When bodies move relative to each other, kinetic friction forces act between their surfaces.

In this study, we have a case of kinetic friction. The friction force does not depend on the size of the contact area and is proportional to the normal reaction force (which is equal to the contact force). The ratio of the maximum friction force T and the reaction force N is called the coefficient of friction:

$$\mu = \frac{T}{N} \tag{1}$$

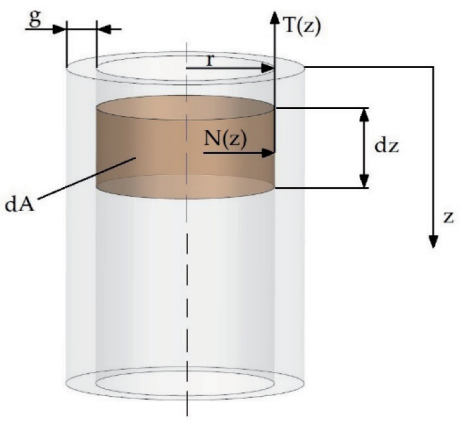

Fig. 8. Model of the distribution of forces inside the mould in the pressing process

Rys. 8. Model rozkładu sił wewnątrz formy w procesie prasowania

To determine the friction force between the die wall and the medium, the values of shear stresses (σ_t) were used (**Fig. 9**).

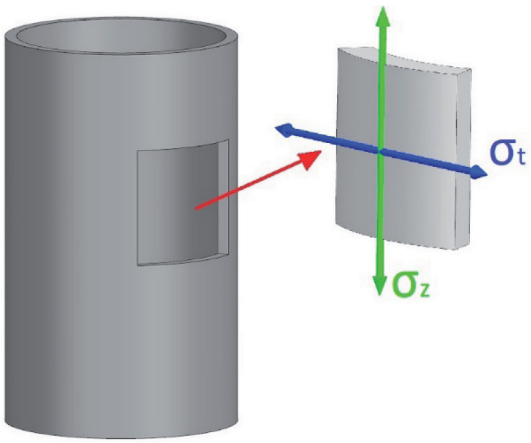

Fig. 9. Distribution of shear and axial stresses on the mould surface

Rys. 9. Rozkład naprężeń stycznych i osiowych na powierzchni formy

The magnitude of these stresses is most often determined based on the Lame formulas, which have the form **[L. 16]**:

$$\sigma_r = \frac{p_a a^2}{b^2 - a^2}\left(1 - \frac{b^2}{r^2}\right) - \frac{p_b b^2}{b^2 - a^2}\left(1 - \frac{a^2}{r^2}\right) \quad (2)$$

$$\sigma_t = \frac{p_a a^2}{b^2 - a^2}\left(1 + \frac{b^2}{r^2}\right) - \frac{p_b b^2}{b^2 - a^2}\left(1 + \frac{a^2}{r^2}\right) \quad (3)$$

However, the above formulas for calculating the stresses in the pipe apply only to pipes with constant internal pressure. In the presented case, the internal pressure is variable in terms of value. The authors, in the work, attempted to determine how the change in internal pressure affects the change of stresses arising on the external surface of the mould and, as a result, the friction force. If so, to what extent. The following analysis will be carried out under conditions where a variable internal pressure is exerted on the mould.

Assuming a variable value of the friction force T(z) as a function of the die height, we can write:

$$T(z) = \mu(z) \cdot N(z) \quad (4)$$

In the above notation, both the variable value of the friction coefficient μ(z) and the normal force N(z) were assumed, depending on the prevailing internal pressure.

Taking into account that the normal force N(z) can be expressed by the product of the internal pressure p(z) and the elementary surface area dA, we obtain:

$$dT = p(z) \cdot dA \cdot \mu(z) \quad (5)$$

Substituting in place of the elementary area dA the expression:

$$dA = 2\pi r \cdot dz \quad (6)$$

where dz is the elementary increment of the mould height, we obtain the elementary value of the friction force:

$$dT = p(z) \cdot \mu(z) \cdot 2\pi r \cdot dz \quad (7)$$

By integrating expression (7), we obtain the friction force in the form:

$$T(z) = 2\pi r \int_0^z p(z)dz \cdot \mu(z) \quad (8)$$

As seen in the expression (8) above, the friction force depends on both the internal pressure value and the friction coefficient.

The value of axial stresses can be written in the form (9):

$$\sigma_z = \frac{T(z)}{2\pi r g} \quad (9)$$

However, the elementary value of the axial stresses can be expressed as:

$$d\sigma_z = \frac{dT}{2\pi r g} \quad (10)$$

Substituting expression (8) into relation (10) we get:

$$d\sigma_z = \frac{\mu(z) \cdot p(z) \cdot 2\pi r \cdot dz}{2\pi r g} \quad (11)$$

and after simplification:

$$\frac{d\sigma_z}{dz} = \frac{\mu(z) \cdot p(z)}{g} \quad (12)$$

Finally, the expression allowing to determine the value of the friction coefficient takes the form (13):

$$\mu(z) = \frac{d\sigma_z}{dz} \cdot \frac{g}{p(z)} \tag{13}$$

Using the equation (13), the value of the coefficient of external friction μ(z) can be indirectly determined depending on the distance from the punch surface. The value of the friction coefficient was determined based on the form of the function σz(z) describing the stress distribution on the outer surface of the matrix, which was obtained in experimental measurements carried out using the resistance strain gauge method, and the function of pressure distribution p(z), which was obtained by analysing images from X-ray tomography. Figure 10 shows the values obtained for the coefficient of external friction as a function of pressure. As can be seen, in the analysed case, the value of the friction coefficient μ(z) decreases with increasing pressure. Because localised high pressures occur during compaction, contact stresses may exceed the yield strength of the material being compacted or the ultimate fracture stress. In this case, the solid particles cannot be considered non-deformable: even if the initial shapes of the particles are regular, these shapes constantly evolve during the pressing process.

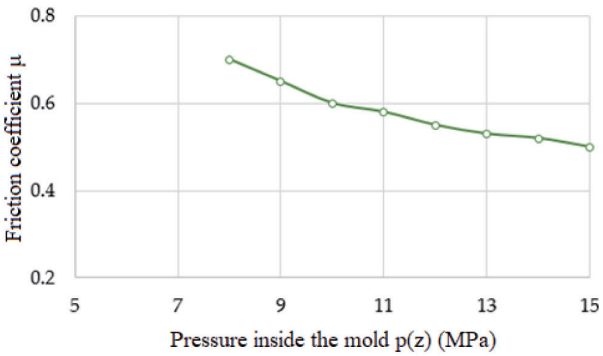

Fig. 10. Dependence of the coefficient of external friction (μ) on the pressure distribution (*p(z)*)
Rys. 10. Zależność współczynnika tarcia zewnętrznego (μ) od rozkładu ciśnienia wewnętrznego (*p(z)*)

For selected areas of the mould, the surface topography was measured using a CNC profilometer Hommel-Etamic T8000RC. **Fig. 11** shows a photograph of the cross-section of the mould used in the tests. The surface topography was measured in five areas, 3 mm long and 3 mm wide.

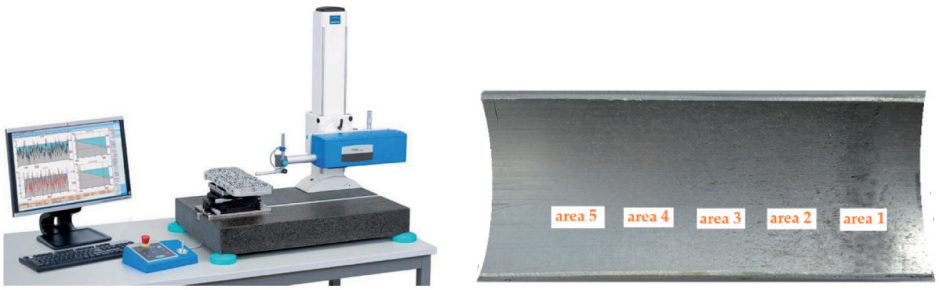

Fig. 11. Stand of surface topography measurement and areas in the die used for the measurement of surface topography
Rys. 11. Stanowisko do pomiaru topografii powierzchni oraz pola w matrycy do pomiaru topografii powierzchni

Surface topography is one of the main features taken into account when evaluating surface quality in bulk material compaction processes. During the tests, the value of the Sq parameter for the surface roughness was measured. The parameter Sq is defined as the root mean square values of surface deviations z(x,y) in the sampling area:

$$\mathrm{Sq} = \sqrt{\frac{1}{\mathrm{A}} \iint_{\mathrm{A}} \mathrm{z}^2(\mathrm{x},\mathrm{y})\,\mathrm{dxdy}} \tag{14}$$

where: A – surface, x, y – lengths in perpendicular directions; z – height position of the x, y surface.

Sq is a statistical parameter with relatively low sensitivity to measurement errors and is often used in surface topography measurements. This parameter is related to the standard deviation of the roughness height, which is often used in contact mechanics.

The topographies of the matrix surface obtained in the compaction process, in places shown in **Fig. 11**, are shown in **Fig. 12**. The value of the Sq parameter was determined based on the topography maps presented in this figure. The presented surface topography maps clearly show that the surface topography changes depending

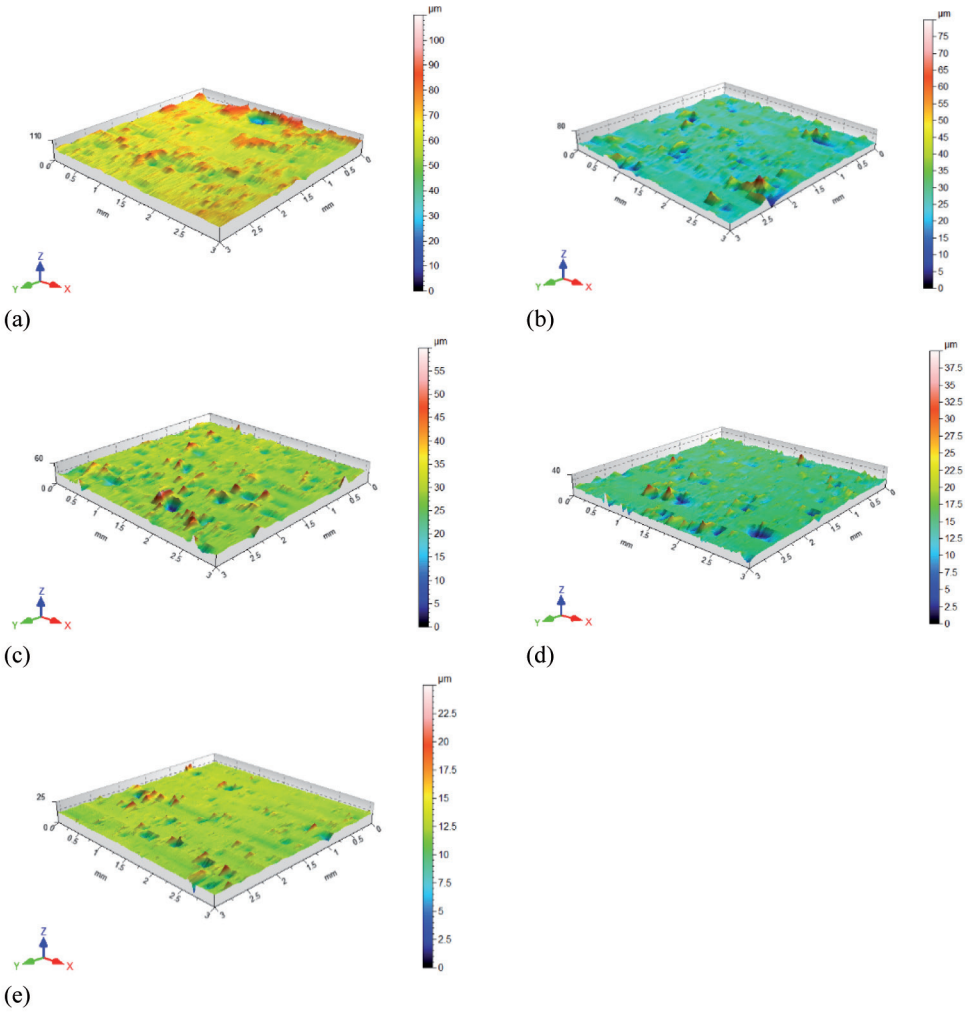

Fig. 12. Surface topography in selected areas of the die surface: (a) area 1; (b) area 2; (c) area 3; (d) area 4; (e) area 5
Rys. 12. Topografia powierzchni w wybranych obszarach powierzchni formy: (a) obszar 1; (b) obszar 2; (c) obszar 3; (d) obszar 4; (e) obszar 5

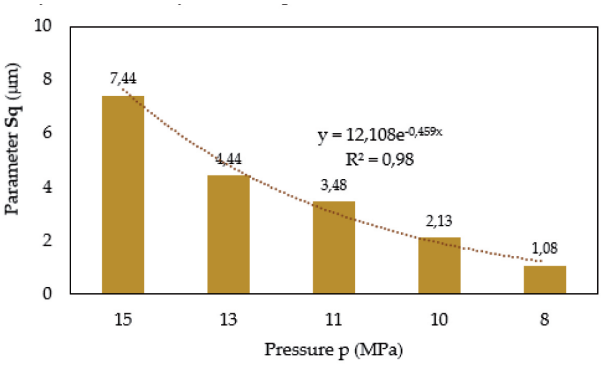

Fig. 13. Effect of the pressure on the root mean square height of the surface
Rys. 13. Wpływ nacisku na parametr *Sq*

on the distance from the punch surface. The first (area 1) and the second (area 2) areas are located in the immediate vicinity of the punch surface, where the highest concentration of silica sand and, at the same time, the highest shear stresses were recorded.

In the surface topography analysis, the Sq roughness parameter was measured separately for five areas of the die surface. **Fig. 13** shows the impact of pressure on the Sq parameter. It can be seen that the change in the value of the Sq parameter is exponential, similar to the pressure distribution in the matrix. The highest value of the Sq parameter occurs near the punch surface, which decreases as you move away from the punch surface.

CONCLUSIONS

As a result of the conducted research and analysis, the following conclusions were drawn:

- changes in the deformation values of the external walls of the mould (both axial and tangential) change exponentially as a function of the distance from the punch. The largest tangential deformations (ε_t) were recorded on the mould's surface near the punch's current position. On the other hand, deformations in the axial direction (ε_z) reached the highest value in the place farthest from the surface of the punch,
- compaction of high-silica sand grains along the punch axis can be described with an exponential function. Layers of sand closer to the surface of the punch are more compacted, which results, among others, from the fact that from a lower value of the coefficient of friction of the compacted material against the inner wall of the mould,
- the tests carried out showed the usefulness of measuring the deformation of the outer surface of the mould for indirect determination of the value of the external friction coefficient,
- distribution of pressure p(z) in the direction of the punch axis during the compaction of high-silica sand can be described by X-ray tomography analysis,
- friction forces cause a drop in pressing pressure with increasing distance from the punch surface,
- the value of the coefficient of friction μ(z) decreases with increasing pressing pressure.

The study of the compaction of high-silica sand of different densities along the matrix height profile will be the subject of future research, the aim of which will be to analyse the inhomogeneity and compaction of the punch and the resulting spatial inhomogeneities for different friction coefficients.

REFERENCES

1. Chtourou H., Guillot M., Gakwaya A.: Modeling of the metal powder compaction process using the cap model. Part I. Experimental material characterization and validation. Int. J. Solids Struct., 39, 2002, 1059–1075.
2. Martin C.L.: Elasticity, fracture and yielding of cold compactem metal powders. J. Mech. Phys. Solids, 52(8), 2004, 1691–1717.
3. Chen M.L., Wu G.J., Gan B.R., Jiang W.H., Zhou J.W.: Physical and Compaction Properties of Granular Materials with Artificial Grading behind the Particle Size Distributions. Adv. Mater. Sci. Eng., 2018, 2018, 8093571.
4. Styks J., Wróbel M., Frączek J., Knapczyk A.: Effect of Compaction Pressure and Moisture Content on Quality Parameters of Perennial Biomass Pellets. Energies, 13, 2020, 1859.
5. Hardman J.S., Lilley B.A.: Mechanisms of compaction of powdered materials. Proc. R. Soc. Lond. A, 333(1593), 1973, 183–199.
6. Lowe C.A., Greenaway M.W.: Compaction processes in granular beds composed of different particle sizes. J. Appl. Phys. , 98, 2005, 123519.
7. Hoffman K.: An Introduction to Measurements using Strain Gauges. Hottinger Baldwin Messtechnik Gmbh: Darmstadt, 1989.
8. Kim K., Kim J., Jiang X., Kim T.: Static Force Measurement Using Piezoelectric Sensors. J. Sensors,, 2021, 2021, 6664200.
9. Żaba K., Trzepieciński T., Rusz S., Puchlerska S., Balcerzak M.: Full-Field Temperature Measurement of Stainless Steel Specimens Subjected to Uniaxial Tensile Loading at Various Strain Rates. Materials, 14, 2021, 5259.
10. Słomiński C., Niedostatkiewicz M., Tejchman-Konarzewski J.: Deformation measurements in granular bodies using a particle image velocimetry technique. Arch. Hydro-Eng. Environm. Mech., 53(1), 2006, 71–94.

11. Hangx S.J.T., Spiers C.J., Peach C.J.: Creep of simulated reservoir sands and coupled chemical-mechanical effects of CO_2 injection. J. Geophys. Res., 115, 2010, 115, B09205.
12. Karner S.L., Chester J.S., Chester F.M., Kronenberg A.K., Hajash A.: Laboratory deformation of granular quartz sand: Implications for the burial of clastic rocks. AAPG Bull., 89(5), 2005, 603– 325.
13. Chuhan F.A., Kjeldstad A., Bjørlykke K., Høeg K.: Experimental compression of loose sands: Relevance to porosity reduction during burial in sedimentary basins. Can. Geotech. J., 40(5), 2003, 995– 1011.
14. Brzesowsky, R.H. Micromechanics of sand grain failure and sand compaction. PhD thesis. Utrecht University: Utrecht, 1995.
15. https://www.kronosedm.pl/aluminium-pa6-aw-2017a
16. Brzoska Z.; Wytrzymałość materiałów. Państwowe Wydawnictwo Naukowe, Warszawa 1972.